www.czasopisma.pan.pl PAN www.journals.pan.pl

ARCHIVES of FOUNDRY ENGINEERING

ISSN (2299-2944)
Volume 18
Issue 2/2018

100 – 104

DOI: 10.24425/122509

17/2

Published quarterly as the organ of the Foundry Commission of the Polish Academy of Sciences

Crystallization Process of Silicon Molybdenum Cast Iron

M. Stawarz
Silesian University of Technology, Department of Foundry Engineering,
Towarowa 7, 44-100 Gliwice, Poland
Corresponding author. E-mail address: marcin.stawarz@polsl.pl

Received 29.01.2018; accepted in revised form 29.03.2018

Abstract

The article presents results of studies of silicon – molybdenum cast iron (4.42% Si, 2.59% Mo and 2.48% C wt.-%) crystallization process. Metallographic analysis was carried out using SEM-scanning electron microscopy with the EDS system. In order to determine the phase composition, X-ray diffraction studies were performed. Thermo-Calc, a computer simulation program, was used to simulate the crystallization process. . The obtained data allowed to describe the effect of some elements on the crystallization process. The silicon phase of MnSi could not be identified during metallographic studies. Also, computer simulation of the crystallization process did not answer the question at which point the silicon phase of MnSi crystallizes in the tested alloy. Therefore, not all results obtained were linked to the registered crystallization process (TDA process). The EDS analysis revealed an unusual distribution of molybdenum in the microstructure of the sample, where it is clearly visible that the area enriched with this element is also the separation of spheroidal graphite. The possibility of occurrence of Mo-rich micro-areas found in graphite is considered. The case is debatable and difficult to resolve at this stage. Perhaps, at such a high concentration of molybdenum (2.59% Mo) in the alloy, conditions are created for simultaneously crystallization of graphite and molybdenum phases.

Keywords: Theory of Crystallization, Metallography, Molybdenum Carbide, Thermal Derivative Analysis, SiMo

1. Introduction

The growing ecological requirements have increased interest in the special. Particularly it comes to work at high temperature for cyclic temperature changes. These working condition are in the new generation of fuel engines are these working conditions. Today's smaller engines are running at higher compression rate and temperature [1]. Castings made of SiMo ductile iron are able to perform and maintain dimensions for many thousands of cycles at elevated temperature [1]. Silicon molybdenum cast iron (SiMo) is suitable for the production of exhaust manifolds, turbines and furnace applications.

The increase in demand for this material causes increased interest in the detailed analysis of its quality, description of the crystallization process parameters and production optimization.
Literature provides data on the crystallization phases in the analyzed alloy, however, the data described are not always unambiguous or there is no confirmation of the obtained results by other researchers. In paper [2], rich phases in Mo were classified as Fe_2MoC-M_6C type carbide phase. Work [3] found the carbides of type M_6C (M = Mo, Si, and Fe).
Mo is found to partly segregate and solidify in intercellular regions, promoting carbides while during the solid state transformation molybdenum particles are precipitated around the

grain boundaries, where small precipitates of Fe_2MoC and in smaller amounts two-phase aggregates of Fe_2MoC/M_6C [4].
Add indentation conditions described in paper [4], Mg was found to segregate to cell boundaries and form $MgSiN_2$ for diesel as well as petrol. In work [5], Mg compounds have been shown that have the ability to segregate at the grain boundaries of the Mo-rich carbide phase, but the phase composition of the Mg rich phase has not been determined. However, in paper [6], carbide phases are described by the authors as "rich molybdenum carbide". Based on the above data, an attempt was made to describe crystallization phases in SiMo cast iron.

SiMo cast iron is also associated with other types of problems that accompany the processes of solidification and crystallization and are associated with the chemical composition of the alloy, mainly the carbon content. The carbon content is lower than in regular ductile iron, i.e., 2.5% - 3.4%. Usually, high carbon content contributes to reducing shrinkage tendency; however, if the carbon equivalent is too high, the iron becomes less fluid and defects looking like cold shuts may be seen [1]. Therefore, common disadvantages of castings of this type of cast iron are, among others, all kinds of shrinkage defects and porosities. An example of a shrinkage porosity for SiMo cast iron is shown in Figure 1.

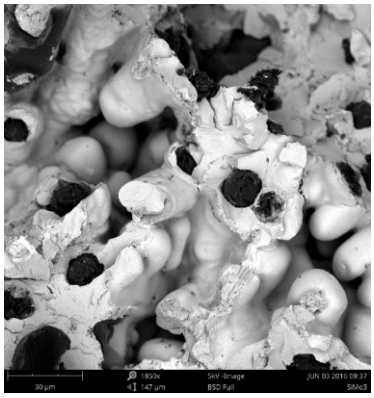

Fig. 1. SiMo cast iron shrinkage porosity. SEM

2. Work methodology and research results

Experimental melts for SiMo iron were performed in the work in accordance with the procedure presented in the works [5, 7]. Experimental melts were conducted in the induction furnace with medium frequency. The charge consisted of steel scrap with low sulphur content. Other ingredients added during the melting was Ranco carburizer, ferrosilicon FeSi75, and FeMo65 rich alloy. The spheroidization process of cast iron was conducted in the bottom of the ladle, after covering the nodulizing agent by pieces of steel scrap. Magnesium rich alloy used in the studies was FeSiMg5RE. Liquid alloy was poured into hot foundry ladle and then poured into shell moulds [5, 7].

In addition, samples were made for microscopic examination using the probe described in the paper [8]. The chemical composition of the tested cast iron was as follows:4.42% Si; 2.59% Mo; 2.48% C; 0.39% Mn; 0.022% P; 0.0097% S; 0.034% Mg.

2.1. Crystallization process analysis

Figure 2 shows the recorded graph of temperature change over time with the calculated first derivative. The thermal effect corresponding to the liquidus temperature is clearly visible. The liquidus temperature value for the tested alloy is 1188 °C. Another thermal effect from crystallization of eutectic is visible for the time interval 111 - 163s, in the temperature range 1111 °C – 1104 °C. At a temperature of 1054 °C, the maximum heat due to the crystallization of Mo-rich carbide phases appears.

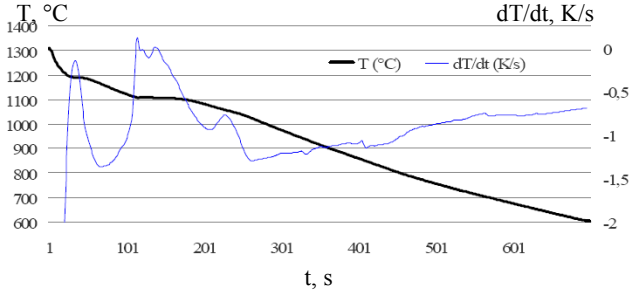

Fig. 2. TDA analysis for SiMo alloy with 2.59% Mo content

Based on the registered TDA course, it can be seen that the leading phase in the crystallization process is austenite. Then, graphite eutectics appear. The next crystallizing phase is the carbide phase or phases (rich in Mo). Obtained results from TDA analysis were confirmed with the results obtained based on computer simulation of the crystallization process (Thermo-Calc). The results of this simulation are presented graphically in Figure 3.

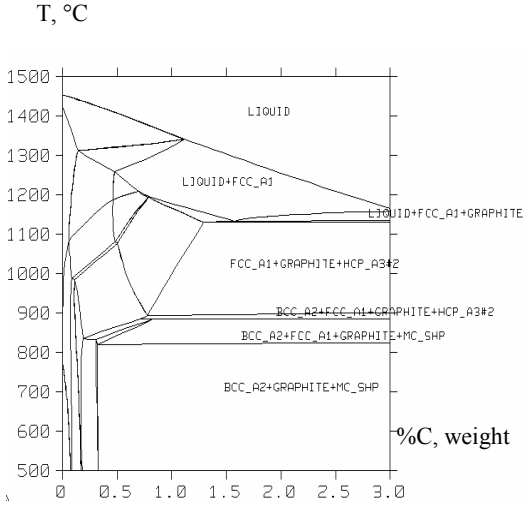

Fig. 3. Computer simulation of the crystallization process. FCC_A1 - austenite. BCC_A2 - ferrite. HCP_A3 # 2, MC_SHP-carbide phases

2.2. X-ray diffraction analysis process

The X-ray diffraction allowed to identify phases forming the alloy. The carbide phases with high amount of molybdenum were defined as Mo_2C molybdenum carbide [9] and phase $Fe_{22}Mo_{12}C_{10}$ (second chemical formula: $Mo_{12}Fe_{22}C_{10}$) as dodecamolybdenum docosairon decacarbide [10]. In analyzed alloy there is also cementite Fe_3C [11] as the component of pearlite. The silicide phase is also present in the sample as MnSi manganese silicide [12]. The results of this analysis were presented in Figures 4-5a, 5b.

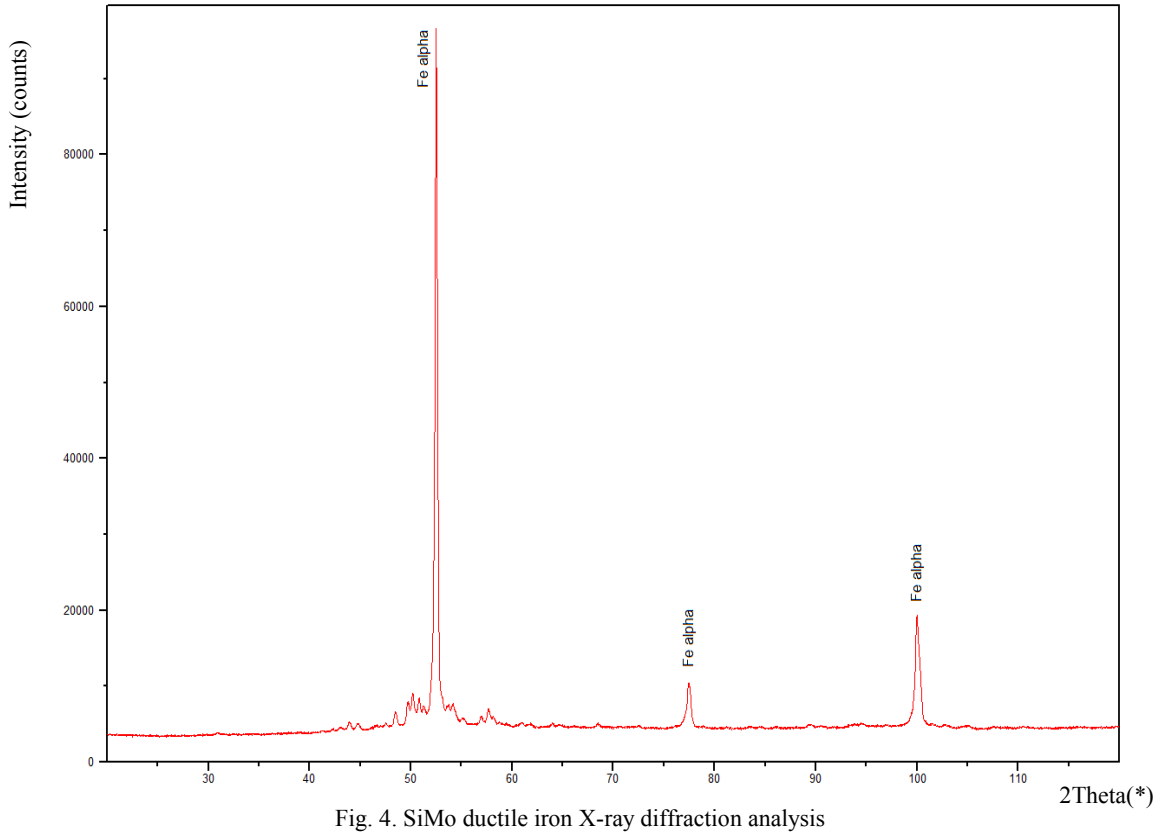

Fig. 4. SiMo ductile iron X-ray diffraction analysis

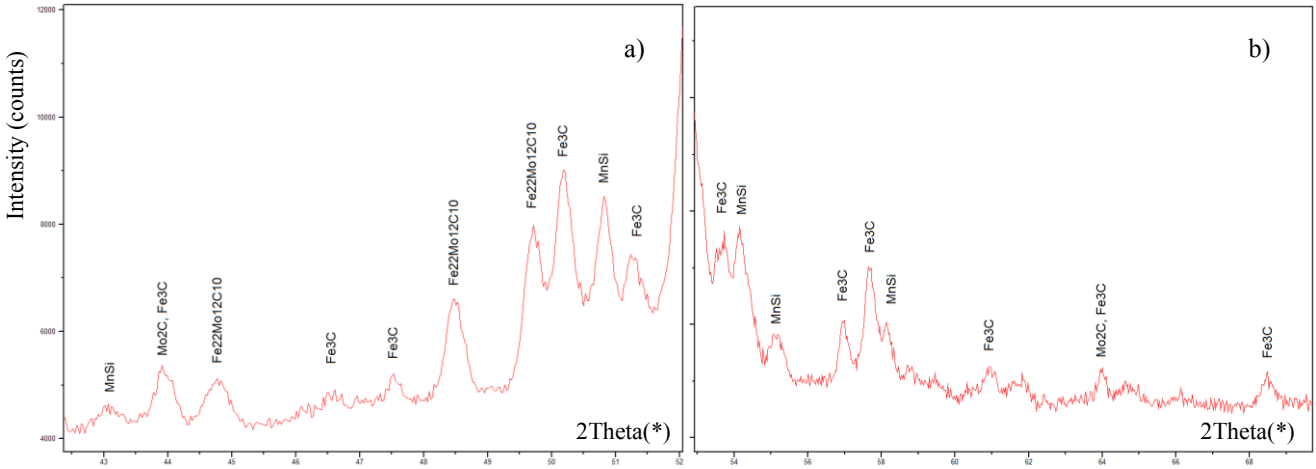

Fig. 5. SiMo ductile iron X-ray diffraction analysis: "a" case for 43 to 52 2Theta(*) angles, "b" case for 53 to 69 2Theta(*) angles

2.3. Metallographic examination

In order to confirm the results obtained from TDA analysis, Thermo-Calc calculations and the X-ray diffraction analysis, metallographic examination were performed using scanning electron microscopy SEM with EDS analysis.

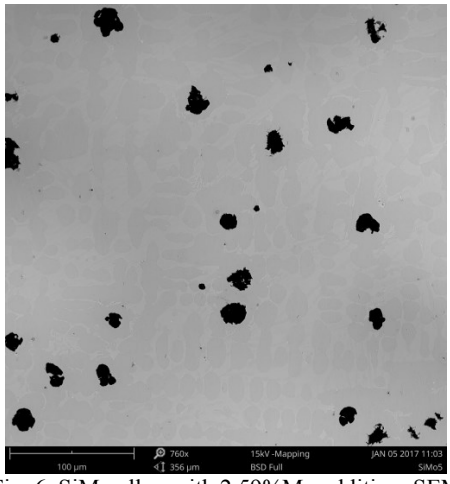

Fig. 6. SiMo alloy with 2.59%Mo addition. SEM

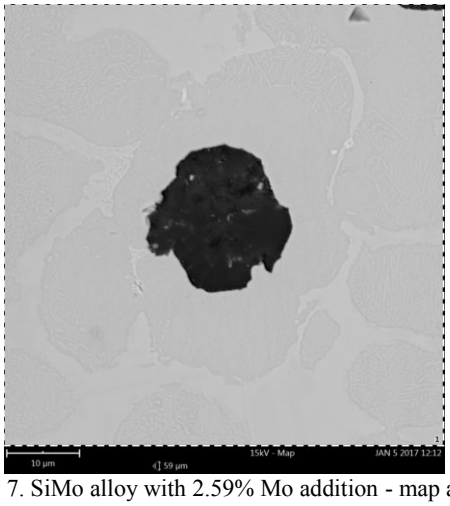

Fig. 7. SiMo alloy with 2.59% Mo addition - map area from EDS system

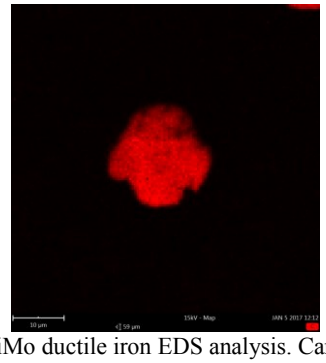

Fig. 8. SiMo ductile iron EDS analysis. Carbon map

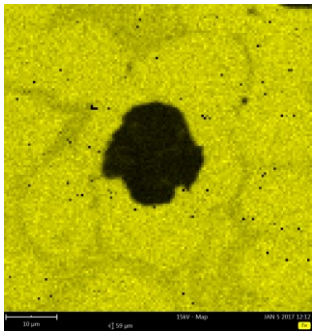

Fig. 9. SiMo ductile iron EDS analysis. Iron map

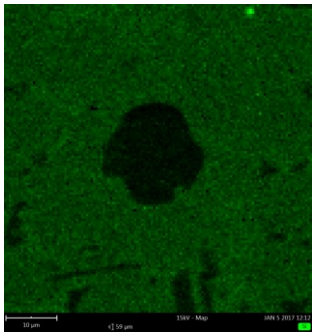

Fig. 10. SiMo ductile iron EDS analysis. Silicon map

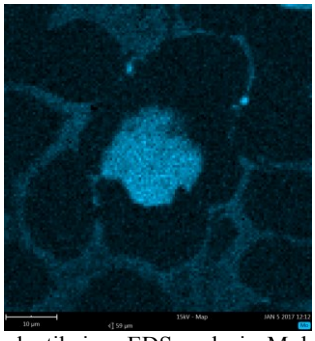

Fig. 11. SiMo ductile iron EDS analysis. Molybdenum map

Figure 6 shows the image of the microstructure of the examined cast iron, while the selected fragment of the microstructure has been enlarged and shown in Figure 7. There is a dark separation of spheroidal graphite, a bright carbide phase (rich in Mo), perlite and ferrite, which surrounds graphite separation.

The EDS analysis (maps of the distribution of elements in Figures 8-11) confirmed the distribution of elements for the studied area. The only exception is the distribution of molybdenum in Figure 11, where it is clearly visible that the area enriched with this element is also the separation of spheroidal graphite. In work [13] the author suggests the possibility of occurrence of Mo-rich micro-areas, which are found in graphite. The case is debatable, at this stage difficult to resolve. In the next step, a breakthrough is achieved by separating the graphite and examining whether the theory of the occurrence of areas rich in Mo is right. It is possible that this high concentration of Mo in the

alloy creates the conditions for simultaneously crystallization of graphite and molybdenum phases

3. Conclusions

Experimental research based on TDA analysis allowed to determine the temperature range corresponding to the crystallization of rich phases in Mo. These results were confirmed based on the simulation of the coagulation and crystallization of the analyzed alloy in the Thermo-Calc program. It was not possible to identify the place of crystallization of the silicon phase MnSi based on computer simulations of the solidification and crystallization process. The X-ray diffraction allowed to identify phases forming the alloy. The carbide phases with high amount of molybdenum were defined as Mo_2C molybdenum carbide [9] and phase $Fe_{22}Mo_{12}C_{10}$ (second chemical formula: $Mo_{12}Fe_{22}C_{10}$) as dodecamolybdenum docosairon decacarbide [10]. In analyzed alloy there is also cementite Fe_3C [11] as the component of pearlite. The silicide phase is also present in the sample as MnSi manganese silicide [12].

Metallographic examinations confirmed the obtained results. However, it was not possible to find the MnSi phase (manganese silicide), on the analyzed samples, although the spectra from this phase are clearly visible on the test results X-ray diffraction.

EDS analysis revealed an unusual distribution of molybdenum (Figure 11), where it is clearly visible that the area enriched with this element is also the separation of spheroidal graphite. In work [13] the author suggests the possibility of occurrence of Mo rich micro-areas, which are found in graphite. The case is debatable, at this stage difficult to resolve. Perhaps, at such a high concentration of molybdenum (2.59% Mo) in the alloy, conditions are created for simultaneously crystallization of graphite and molybdenum phases. .

References

[1] Roedter, H. (2006). 4–6% Silicon ductile irons for high temperature service. Sorelmetal. Rio Tinto Iron& Titanium inc.

[2] Li, D. & Sloss, C. (2015). Heat treatment of heat-resistant ferrous cast alloys. *International Journal of Metalcasting.* 9(2), 7-20.

[3] Mervat, M.I., Nofal, A. & Mourad, M.M. (2016). Microstructure and hot oxidation resistance of SiMo ductile cast irons containing Si-Mo-Al. *Metallurgical and Materials Transaction B.* DOI 10.1007/s11663-016-0871-y

[4] Magnusson Åberg, L. & Hartung, C. (2012). Solidification of SiMo nodular cast iron for high temperature applications. *Trans Indian Inst Met.* 65(6), 633-636. DOI 10.1007/s12666-012-0216-8.

[5] Stawarz, M. (2017). SiMo ductile iron crystallization process. *Archives of Foundry Engineering.* 17(1), 147-152. DOI: 10.1515/afe-2017-0027.

[6] Hervas, I., Thuault, A. & Hug, E. (2015). Damage analysis of a ferritic simo ductile cast iron submitted to tension and compression loadings in temperature. *Metals.* 5, 2351-2369. DOI:10.3390/met5042351.

[7] Stawarz, M., Nuckowski, P.M. & Dojka, M. (2017). High molybdenium silicon cast iron crystallization process. In Metal 2017: 26th International Conference on Metallurgy and Materials – Metal 2017. Ostrava: TANGER 2017, 229-234.

[8] Wilk-Kolodziejczyk, D., Regulski, K. & Gumienny, G. (2016) Comparative analysis of the properties of the nodular cast iron with carbides and the austempered ductile iron with use of the machine learning and the support vector machine. *The International Journal of Advanced Manufacturing Technology.* 87, 1077-1093. DOI: 10.1007/s00170-016-8510-y.

[9] Ouahrani, T., Faraoun, H.I. & Abderrahim, F.Z. (2012). Structure, bonding and stability of semi-carbides M_2C and sub-carbides M_4C (M=V, Cr, Nb, Mo, Ta, W): A first principles investigation. *Physica B, Condensed Matter.* 407, 3833-3838, DOI: 10.1016/j.physb.2012.05.070.

[10] Nowotny, H.N., Wayne, S.F., Kostiner, E. & Rapposch, M.H. (1983). *Revue de Chimie Minerale.* 20, 528-531.

[11] Wood I.G., Vocadlo L., Knight, K.S., Dobson D.P., Marshall, W.G., Price, G.D. & Brodholt, J. (2004). Thermal expansion and crystal structure of cementite, Fe_3C, between 4 and 600 K determined by time-of-flight neutron powder diffraction. *Journal of Applied Crystallography.* 37, 82-90. DOI: 10.1107/S0021889803024695.

[12] Shoemaker, D.P. & Brink-Shoemaker, C. (1971). *Acta Crystallographica B* (24,1968-38,1982), 27, 227-235.

[13] Stolarz, S., Rutkowski, W. (1961) *Tungsten and molybdenum.* Warsaw: State Technical Publishing. (in Polish).